Conformational analysis of some pyridinium phenolates and synthetic precursors based on X-Ray and IR characterisations

Hélène Chaumeil[a*)], Markus Neuburger[b)], Patrice Jacques[c)], Théophile Tschamber[d)], Vincent Diemer[a)], Christiane Carré[e)]

[a)] Laboratoire de Chimie Organique et Bioorganique, Université de Haute Alsace, Ecole Nationale Supérieure de Chimie de Mulhouse, Institut Jean-Baptiste Donnet, 3 bis rue Alfred Werner, 68093 Mulhouse Cedex, France.

[b)] Laboratory of Chemical Crystallography, Department of Chemistry, University of Basel, Spitalstraβe 51, 4056 Basel, Switzerland.

[c)] Laboratoire de Photochimie et d'Ingénierie Macromoléculaires, Université de Haute Alsace, Ecole Nationale Supérieure de Chimie de Mulhouse, Institut Jean-Baptiste Donnet, 3 bis rue Alfred Werner, 68093 Mulhouse Cedex, France.

[d)] Laboratoire de Chimie Moléculaire, CNRS, UMR 7509, Université de Strasbourg, Ecole Européenne de Chimie, Polymères et Matériaux, 25 rue Becquerel, 67087 Strasbourg, France.

[e)] CNRS, Laboratoire Foton (UMR 6082), ENSSAT, 6 rue de Kerampont, CS 80518, 22305 Lannion Cedex, France.

Abstract:

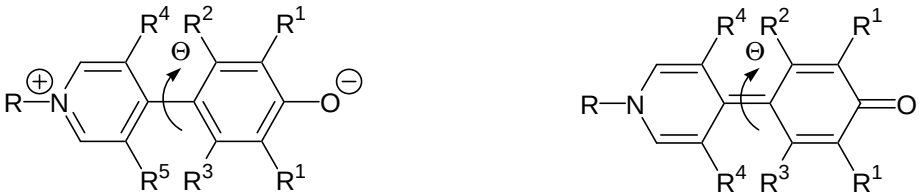
This manuscript reports X-Ray and IR characterizations of representative pyridinium phenolates, model compounds for nonlinear optics. These analyses reveal the close dependence existing between molecular structure and the contribution of quinone and zwitterionic limiting forms. The bond length alternation (BLA) values, the well-known parameter correlated to hyperpolarisability β, are also discussed and compared with literature data.

1- Introduction

Π-conjugated derivatives that possess an electron donor group at one end and an electron attracting group at another end, usually called push-pull compounds have attracted much attention because of their interesting optical properties, as well as the opportunity they give for a fundamental understanding of the interaction between these compounds and light. Among push-pull molecules, the biphenyl derivatives present a special enticement due to the ability of phenyl rings to rotate around intercyclic bond. The variation of twist angle induces a modulation of the charge transfer between the two aromatic parts of the molecule in the particular case of biphenyls with a zwitterionic character, that is, for molecules with a ground state dominated by a charge separated resonance form.[1-10] Their interaryl twist angle is readily tuned by introducing sterically hindered substituents at *ortho-ortho'* positions of the intercyclic bond.

A particular attention has been paid to pyridinium phenolates as model structure of twisted intramolecular charge transfer molecules, that is, in other word TICTOID,[7-15] their ground state geometry being represented as a linear combination of zwitterionic and quinoïd resonance structures (Scheme 1).[16-17]

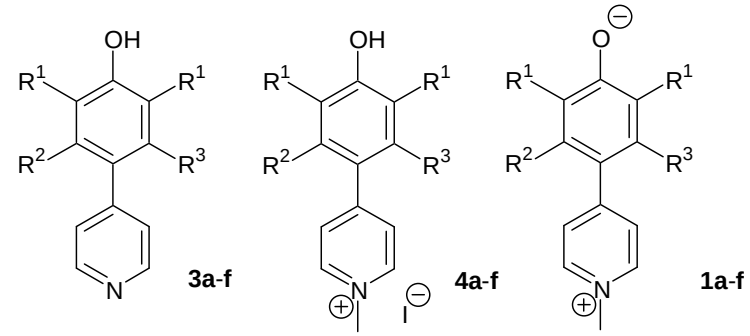
In the present manuscript, the solid-state structures elucidated by X-ray diffraction analysis of representative pyridinium phenolates and some of their synthetic precursors, as well as IR analysis, are reported. Furthermore, we study the dependence existing between molecular structure and contribution of the two limiting forms related to the two pyridinium phenolates series.

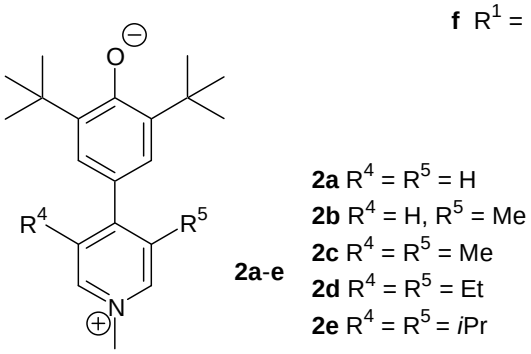


Scheme 1: Limiting forms (zwitterion and quinone).

2- Discussion

We have earlier reported the synthesis of two pyridinium phenolate series **1a-f** and **2a-e** (Scheme 2) sterically crowded by alkyl substituents at *ortho* positions of the interaryl bond.[18-19] The two synthetic pathways used are quite similar. However, in the particular case of **1a-f**, the last two steps were the *N*-alkylation of pyridinyl phenols **3a-f** and the cautious deprotonation of **4a-f**.

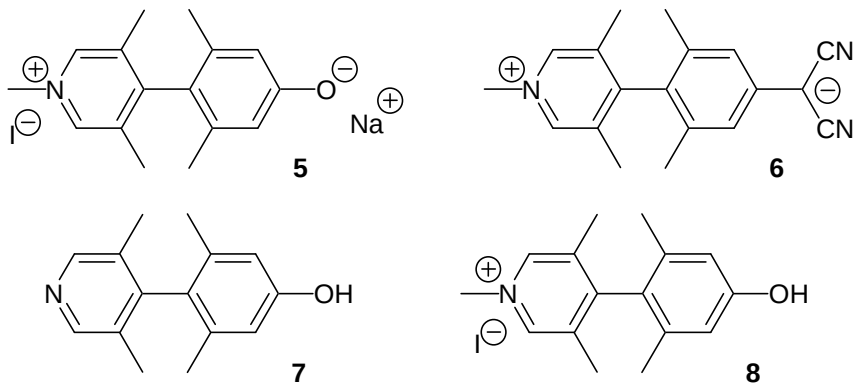




Scheme 2: Compounds **1a-f**, **2a-e**, **3a-f** and **4a-f**.

The low solubilities of **1a-f** have prevented their non-linear optical (NLO) characterizations.[20] However, the introduction of bulky *tert*-butyl groups at *ortho* position of the phenolate function reduces the formation of aggregates and significantly enhanced the solubilities of **2a-e**. Experimental measurements of NLO properties of **2a-d** with twist angle achieving 50° have confirmed the predicted enhancement in quadratic response with the raise of twist angle.[10]

It is worth recalling here that many theoretical studies, as well as experimental measurements concerning the optical properties of various pyridinium phenolates, have been conducted since the early 90's. In particular, sustained efforts have been exerted to design chromophores with ever-stronger NLO responses.[3, 6, 8, 11-13, 21-25] Recently, the synthesis of **5** and **6** crowed by four methyl groups at *ortho-ortho'* positions of the intercyclic bond was achieved (Scheme 3).[11-13] Unfortunately, the too low solubility of **5** makes its NLO characterization impossible. **6** possesses a strong electron accepting dinitrile function and exhibits hyperpolarizabilities that are an order of magnitude above the best performing conventional chromophores to date. Exaltation of NLO response is attributed to the interplay of three configurations, which include, beside the neutral and the zwitterionic forms, a biradical one. Unfortunately, the large dipole moments of these derivatives **5** and **6** lead to high aggregation propensities. Their biradical character compromises their chemical stability and as a consequence seriously limits their use in integrated optical devices.

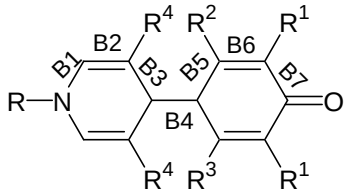


Scheme 3: Marks's group derivatives.[11-13]

2.1- X-ray results

The X-ray structures of compounds **5** and **6** as well as those of their synthetic intermediates have been published.[11-13] Thus, the comparison of the structure of some of our intermediates and pyridinium phenolates with those of Marks's group is of great interest in order to evaluate the structural changes induced by the torsion and the different functionalities anchored on the molecule backbones.

Line	compounds	B1	B2	B3	B4	B5	B6	B7	C-O	Θ	Θ[a)]	BLA[b)]	BLA[i)]
1	**3e**	1.335	1.379	1.390	1.490	1.397	1.390	1.387	1.364	81.5			
2	**3f**	1.332	1.385	1.385	1.496	1.403	1.4015	1.393	1.379	76			
3	**7**	1.331	1.391	1.401	1.493	1.401	1.390	1.393	1.358	85.7			
4	**4a**	1.445	1.364	1.396	1.472	1.395	1.388	1.386	1.363	23.9			
5	**4c**	1.342	1.365	1.399	1.481	1.404	1.390	1.385	1.363	55			
6	**4d**	1.335	1.381	1.390	1.490	1.405	1.397	1.386	1.374	75.4			
7	**8**	1.338	1.383	1.396	1.497	1.400	1.392	1.391	1.364	86.1			
8	**1a**	1.350	1.369	1.409	1.457	1.411	1.377	1.421	1.262	5.7		0.039	0.013
9	**1a**[c)]	*1.385*	*1.366*	*1.447*	*1.379*	*1.449*	*1.448*	*1.467*	*1.243*				*0.057*
10	**1a**[d)]	*1.375*	*1.361*	*1.446*	*1.411*	*1.443*	*1.362*	*1.464*	*1.244*				
11	**1a**[e)]	*1.375*	*1.359*	*1.445*	*1.408*	*1.444*	*1.359*	*1.466*	*1.234*		*0*	*0.093*	*0.076*
12	**5**[e)]	*1.368*	*1.372*	*1.446*	*1.442*	*1.450*	*1.371*	*1.454*	*1.246*		*56.91*	*0.079*	*0.055*
13	**5**[f)]	1.345	1.383	1.402	1.489	1.406	1.387	1.411	1.312	86.9		0.021	-0.013
14	**6**[g)]	1.339	1.377	1.406	1.501	1.406	1.388	1.401				0.019	0.016
		1.3445	1.380	1.404	1.492	1.405	1.3825	1.401					
15	**2a**	1.353	1.356	1.424	1.429	1.419	1.365	1.462	1.262	11.0		0.073	0.052
16	**2a**[h)]				*1.410*				*1.257*		*12*		
					(1.380)				*(1.244)*		*(0)*		
17	**2b**	1.352	1.363	1.408	1.446	1.402	1.370	1.457	1.267	28.9		0.054	0.029
18	**2b**[h)]				*1.423*				*1.261*		*35*		
					(1.384)				*(1.245)*		*(23)*		



[a] Calculated angles in solution (in gas phase).
[b] BLA = [(B3-B2)+(B5-B6)+(B7-B6)]/3 (reference[25]).
[c] Calculated values.[3]
[d] Calculated values.[27]
[e] Calculated values.[25]
[f] **5** crystallized with NaI. Experimental values.[11-13]
[g] Experimental values. There are two independent molecules of **6** in the unit cell.[11-13]
[h] Calculated values in CH_3CN[10] (or in gas phase).
[i] BLA = [(B3-B2)+(B5-B4)+(B7-B6)]/3 (this work).

Table 1: Average of bond lengths (Å), twist angle (°) from X-Ray analysis (present work) or literature values (experimental or theoretical) and bond length alternation values (BLA) of twisted pyridinium phenolates studied. All theoretical values and their corresponding BLA are in italics.

As expected, the X-ray structures of **3e** and **3f** clearly indicate a classic aromatic framework (Table 1). Their ORTEP (Oak Ridge Thermal Ellipsoid Plot) representations are shown in Table 2. All aromatic bonds are of similar lengths and the distance of intercyclic bond (around 1.49 Å) matches with this of biphenyl (1.515 Å).[26] The two aryl moieties are twisted out of plane. The angle values are, respectively equal to 81.5° and 76°. All these structural features**,** except for dihedral angle, are very close to those of **7**, precursor of **5** (Table 1, entry 3).

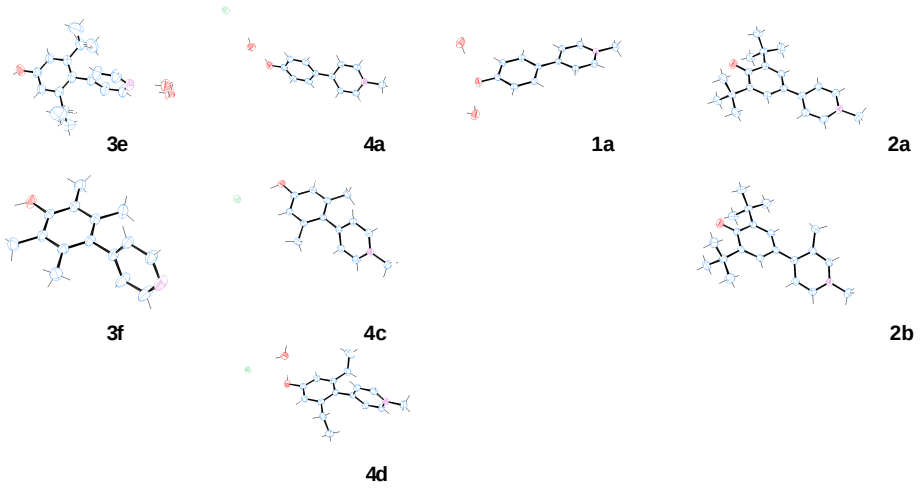


Table 2: ORTEP diagram of compounds **3e,f**, **4a-d** and **2a-b**.

The architecture of biaryliodide salts **4a**, **4c** and **4d** also respect an aromatic biaryl framework. Once again, the same structural data can be drawn from the X-ray structure of Marks's **8** intermediate (Table 1, entries 4-7).

The X-ray analysis of the two series of pyridinium phenolates must be considered independently. Compounds **1a**, **5** and **6** crystallize in a monoclinic crystal system: **1a** with two molecules of water, **6** with molecules of water and acetone, **5** as complexes with NaI units. The strong affinity of Na^+ with the phenolate oxygen atom of **5** leads to a head to head arrangement of two molecules linked by a Na^+ cation. The crystal packing of this

chromophores consists in a centosymmetric dimer of two dimeric complexes linked between two neighbouring pyridinium phenolates from each complexes arrayed in an antiparallel fashion.[12] This last feature together with the presence of a hydrogen bond between water and charged oxygen atom of **1a** or the charged carbon of malonodinitrile moiety of **6** promotes the zwitterionic forms, as shown in our solvatochromism studies dealing with compounds **2a-e**.[17] On the other hand, **2a** and **2b** crystallize in orthorhombic crystal system without any co-crystallized molecule or cation.

All experimental intercyclic bonds and C-O distances of compounds **1a**, **2a**, and **2b** (Table 1, entries 8, 15, 17) are slightly shorter than those of pyridinyl phenols and pyridinyl phenol salts (Table 1, entries 1-7). However, it should be especially noted that these bonds are shorter than typical simple intercyclic biphenyl (1.478[26]) and C-O bonds, and longer than C=O quinone double bonds (1.222Å[26]). It is probably a result of the contribution of quinone limiting form to ground state. However, these bond lengths increase as the twist angle increases displaying the lessening of the conjugation. As a result, **5** respectively **6**, whose positive and negative charges are properly localized on pyridinium nitrogen and either on phenolate or on the charged carbon of malonodinitrile moiety, exhibit significantly less quinoïdal character than **1a** respectively **2a**.

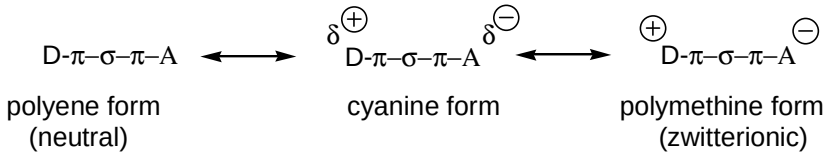
Calculated aromatic bond lengths of **1a** are alternately shorter or longer[3, 25, 27] than those derived from X-ray analysis (Table 1, entries 8-11). Besides, the intercyclic and C-O calculated bond lengths are all underestimated, indicating the too large contribution of the quinone limiting form in calculations. Such an underestimation of calculated bond lengths is depicted for compounds **5** and **2a-b** (entries 12-13 and 15-18).[25, 10] Nevertheless, twist angles existing between the two aromatic rings of **2a-b** match well with those obtained by semi-empirical measurement (entries 15-18).[10]

2.2- **Discussion about bond length alternation (BLA)**

The fact, that quadratic hyperpolarisability β has been correlated to the bond length alternation (BLA) parameter,[28-31] prompted us to investigate it for representative molecules reported in Table 1. BLA is defined as the average length differences between single and double bonds in polyene chains. Thus, in the case of D-π-A molecules, BLA is positive for neutral form, zero for the cyanine limit structure and negative for the zwitterionic contributor. It should be noted that some authors adopt the opposite convention.[32] Interestingly, it was recently shown that the sign of BLA could be inversed as the length of polyene chain increased.[32]

Our main objective is to determine to what extend the torsion angle could modify the structure. However, we first should pay attention to the fact that the presently studied heterocyclic betaines are not typical donor-acceptor π conjugated molecules. Their charge transfer (CT) electronic transition arises owing to the interaction of the different π orbitals present in the D, A moieties through the σ bonds of the biphenyl core (Scheme 4). Moreover, the above mentioned classification of BLA is - strictly speaking - only valid for planar molecules. However, we contend that the BLA values reported in Table 1 can be predictive of the structures studied here. More importantly, these BLA values considered in a comparative approach can give valuable information about both the dependence of the structure on the torsion angle and the change induced by solvatation, compared to the X-ray data corresponding more or less to non polar solvent. In addition, it should be mentioned that the BLA calculation is not straightforward. The formula used here (BLA = [(B3-B2)+(B5-B4)+(B7-B6)]/3), where bonds are numbered starting from nitrogen-carbon bond B1 to carbon-oxygen bond B8, B4 being the C-C intercyclic bond) (Table 1), seems us the most appropriate and differs considerably from the one reported by Liu.[25] Finally, some compounds bear methyls at *ortho* position of the intercyclic bond in order to tune the steric hindrance.

Fortunately, these substituents correspond to low Hammett constants and are not taken into account when calculating the BLA, as recently performed in our paper on solvatochromism[17]. With these restrictions in mind, the following discussion reveals interesting features.



Scheme 4: Ground state of pyridinium phenolate molecule viewed as a combination of two valence-bond (VB) forms. (Note the presence of a σ bond in the molecules studied here).

From our X-ray analysis, the model compound **1a** has a BLA value of 0.013 (entry 8) corresponding to a moderate quinone type structure, confirmed by its short C=O length of 1.262 Å. Interestingly, the strongly twisted compound **5** reported by Ratner et al.[11-13] has a negative value of BLA (-0.013) (entry 13). These features clearly point out that the torsion modifies significantly the structure towards a zwitterionic one. This is also confirmed by the consequent elongation of the C=O bond, this length being now of 1.312 Å.

Now, comparing **2a** and **2b**, we observe that the increasing torsion (from 11° to 28.9°) decreases the BLA (from 0.052 to 0.029) concomitantly to a very small increase of carbonyl bond length (from 1.262 to 1.267 Å) (entries 15 and 17). Consequently, **2b** has still a quinone type structure. Unfortunately, it was not possible to get good quality crystals of **2c**, **2d** and **2e**.

Further, inspection of Table 1 reveals that calculated bond lengths can drastically be different, depending on the level of quantum chemistry approach. This remark underlines the failure of quantum chemistry to describe properly these structures (entries 9, 10, 11, 12, 16, 18). Anyway, the formula for BLA used by Liu et al.[25] seems inappropriate by considering the very small decrease of BLA (from 0.093 to 0.079), when going from **1a** to **5,** and the fact that **5** has a too high positive value for such a twisted molecule.

Finally, the present investigation puts in light the fact that the low value of BLA for **1a** (0.013), indicative of a very moderate polar structure, is in contradiction with the strong blue shift solvatochromism of its UV absorption, recently reported.[17] Indeed, the **1a** solvatochromism relies on a high decrease of the factor $\mu_g(\mu_e-\mu_g)$ (μ_g and μ_e being respectively the dipole moments of the ground and Franck Condon states).[10] This implies a high value of μ_g and a consequent decrease of μ_g upon excitation, apparently in contradiction with a cyanine like structure having a small dipole moment. But, we propose to level off this contradiction by admitting that solvatation is strong enough to induce structural changes towards a zwitterionic form. Indeed, such a structure undergoes an intense blue solvatochromism, as exemplified by the empirical parameter $E_T(30)$.

2.3- IR results

The IR spectra of compounds **2b-e** recorded in solid-state (KBr pellet) are shown in Figure 1. All derivatives exhibit sharp intense bands in the 1000-1700 cm^{-1} region. Among these transitions, many of them can be easily assigned knowing that the IR spectrum of **2a** has been theoretically and experimentally thoroughly studied in the past.[6,8] The band around 1200 cm^{-1} corresponds to the methyl-*N* stretch while this around 1325 cm^{-1} is ascribed to the intercyclic C-C stretches between pyridinium and phenoxide rings. The transition around 1580 cm^{-1} mainly corresponds to the quinoïdal double bond stretch, combined with a slight contribution of pyridinium stretch and ring carbon-carbon stretching vibrations. The band around 1640 cm^{-1} mainly corresponds to a pyridinium stretch. This interpretation differs from this of Ratner, but is confirmed by literature[6,8] and by comparison between IR spectra of pyridinyl phenols and pyridinium salts, precursors of **2a-e**. [18-19] Actually, the band around 1600-1640 systematically lacks for all the spectra of pyridinylphenols but exists in all the spectra of pyridinium salts. It must be added that the CH_3 bending of *tert*-butyl groups is commonly

observed as a doublet around 1385-1395 cm^{-1} and 1370 cm^{-1} while the degenerated bending give raise to a strong band at around 1400 cm^{-1}.[33] Bands are actually observed at 1402 and 1361 cm^{-1} in the FTIR spectrum of 2,4-di-*tert*-butylphenol [33] and at 1390 and 1370 cm^{-1} in the case of 3,3',5,5'-tetra-*tert*-butyldiphenylquinone.[34-35] In contrast, the spectrum of **2a** exhibit only a single sharp band at 1393 cm^{-1}.[19] Two bands are again observed for **2b-e** (around 1414-1420 cm^{-1} and 1373-1378 cm^{-1}). This explains why all spectra are normalized in absorbance taking the transition at 1410-1420 cm^{-1} as a reference. As usual, the frequency region 1350-1430 cm^{-1} remains not further interpreted.

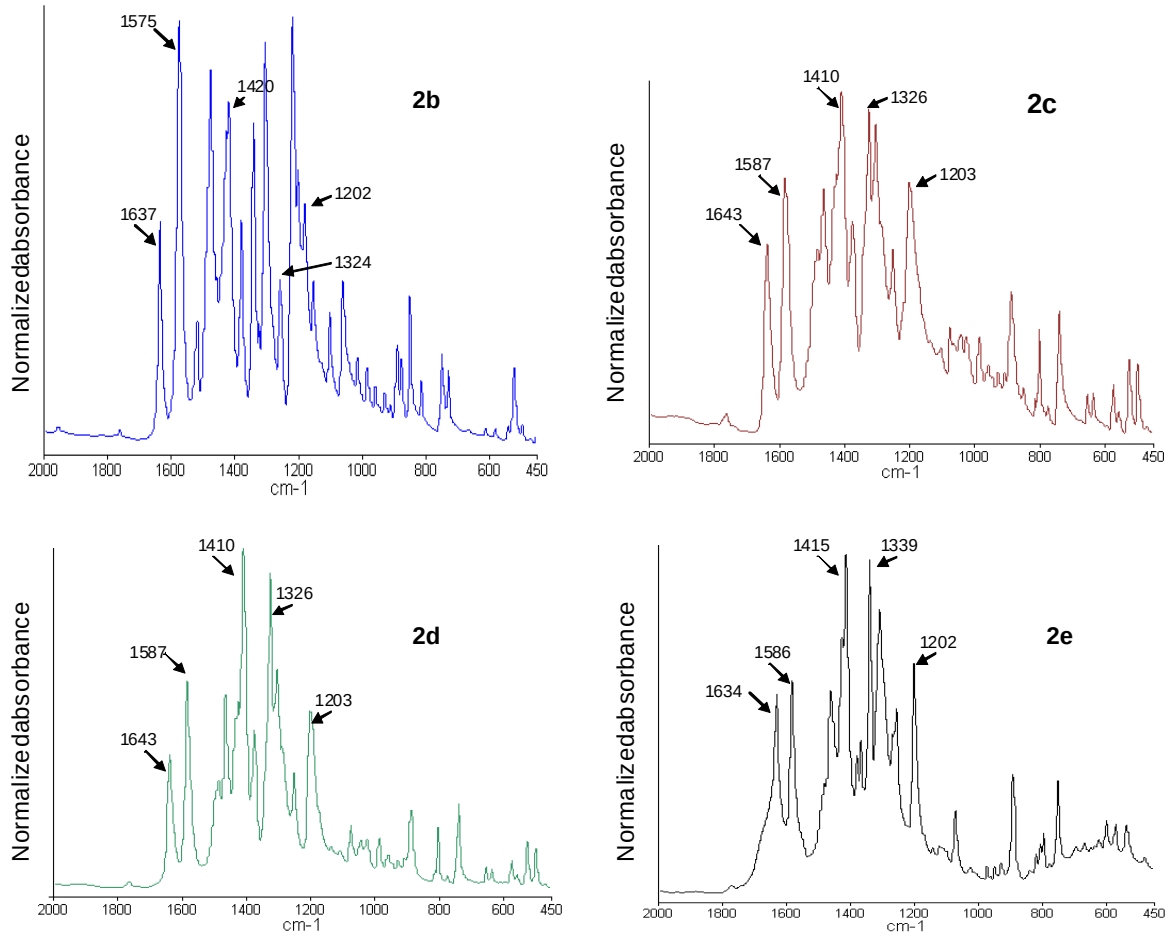


Figure 1: IR spectra of compounds **2b-e** as KBr pellet. (All spectra were normalized in absorbance taking the transition at 1410-1420 cm^{-1} as reference).

The transition located around 1325 cm^{-1} (intercyclic C-C stretching) can be expected to be sensitive to the twist angle variations. Unfortunately, band superposition and likely covering with C-O stretching vibration make undetectable any change in bond intensity. The C=O stretching mode (ν(C=O)) around 1580 cm^{-1} has a different behaviour despite the weak contribution of pyridinium stretch. A decrease of the intensity of this transition from **2b** to **2d** is expected, arguing for the lowering contribution of the quinoïdal limiting form as the twist angle raises. Such a decrease is observed going from **2b** to **2c**. The torsion angle for **2c** and **2b** being very close (tables 3), the intensity decrease of ν(C=O) from **2c** to **2d** is logically extremely weak. At the same time, as it might be expected and in agreement with literature,[36] an increase of the wavenumber with the torsion. This well-known hypsochromic effect is easily explained by the increase in bond strength as the conjugation vanishes. Actually, in the present work, with the torsion and the concomitant decrease in conjugation, the wavenumber increases from 1575 cm^{-1} for **2b** to 1587 for **2c** or**2d**. The interpretation of **2e** spectrum is trickier, since *iso*-propyl and *tert*-butyl groups give similar characteristic doublets in the symmetric CH_3 bending region. However, the band located at 1586 cm^{-1} would be less intense than this at 1587 cm^{-1} in the case of **2d**, once the *iso*-propyl contribution deduced.

Attempt to transpose this study to compounds **1a-e** is so far not feasible. Any increase in twist angle affects all stretching and bending mode. As a consequence, no method of standardisation can be obviously proposed.

	2a	**2b**	**2c**	**2d**	**2e**
δ(*tert*-butyl) /ν(C=O)		0.40	0.68	0.72	0.80
Θ	12	35	45	48	54

Table 3: Bands absorption ratio's of δ(*tert*-butyl) to ν(C=O) and twist angles obtained from numerical simulations.[10]

3- Conclusion

All considered synthetic intermediates correspond to aromatic structures. In contrast, the shift and intensity variations of IR bands, being in agreement with BLA variations, confirm firstly, that quinoïde and zwitterionic limiting forms contribute to the ground state structure of pyridinium phenolates; secondly, that the zwitterrionic form becomes predominant, as the twist angle increases. Finally exploring potential applications for nonlinear optics, it should be kept in mind that the solvent or, generally speaking, the medium can modified drastically the conformation of these molecules.

4- Experimental part

The synthesis of studied compounds was previously described.[18-19]

All X-Ray structures were determined from single crystals obtained by slow evaporation of acetonitrile solutions. The suitable samples were analysed on a Nonius Kappa CCD diffractometer at 173K using graphite-monochromated Mo K_α-radiation with λ = 0.71073 Å. The Nonius suite was used for data collection and integration. The structure was solved by direct methods using the program SIR92.[37] Least-squares refinement against F was carried out all non-hydrogen atoms using the program CRYSTALS.[38] Chebychev polynomial weights were used to complete the refinements. Plots were produced using CAMERON.[39] Space group, lattice parameters and other relevant information are listed in Table 4. Crystallographic data, excluding structure factors, for the structures in this paper were deposited with the Cambridge Crystallographic Data Center. Crystallographic Data Center. CCDC 768158 to 768162 contain the supplementary crystallographic data for, respectively **3f**, **4c**, **1a**, **2a** and **2b**, CCDC 983983 to 983985 the supplementary crystallographic data for **3e**, **4d** and **4a**. Copies of the data can be obtained, free of charge, on application to the CCDC, 12 Union Road, Cambridge CB2 1EZ, UK [fax: +44-1223-336033 or e-mail: deposit@ccdc.cam.ac.uk].

IR spectra were recorded on a Perkin-Elmer spectrum 65 FTIR spectrometer. **2b**: IR (KBr): ṽ = 1637, 1575, 1476, 1428, 1420, 1381, 1344, 1323, 1303, 1213, 1202, 1180 cm^{-1}. **2c** : IR (KBr): ṽ = 1643, 1587, 1466, 1425, 1410, 1373, 1326, 1304, 1203 cm^{-1}. **2d** : IR (KBr): ṽ = 1643, 1587, 1487, 1466, 1425, 1410, 1373, 1326, 1304, 1251, 1203 cm^{-1}. **2e** : IR (KBr): ṽ = 1634, 1586, 1469, 1428, 1415, 1379, 1367, 1257, 1201 cm^{-1}.

Compounds	**3e**	**3f**	**4a**	**4c**	**4d**
Chemical formula	$C_{15}H_{19}N_1O_2$	$C_{15}H_{17}N_1O_1$	$C_{12}H_{14}INO_2$	$C_{14}H_{16}INO$	$C_{16}H_{22}I_1N_1O_2$
Formula weight	245.32	227.31	331.15	341.19	387.26
Crystal appearance	Colourless plate	Colourless plate	Colourless plate	Colourless plate	Colourless plate
Size mm^3	0.12·0.28·0.28	0.13·0.28·0.32	0.04·0.10·0.20	0.12·0.20·0.29	0.10·0.16·0.21
Crystal system	Trigonal	Monoclinic	Orthorhombic	Monoclinic	Orthorhombic
Space group	R -3c	P 21/c	P 21 21 21	P 21/a	P c a b
Unit cell dimensions Å	a = 16.3055(5), b = 16.3055(5) c = 27.6692(10)	a = 8.5707(4) b = 9.6582(4) c = 15.7429(7)	a = 7.13960(10), b = 10.2823(2) c = 17.1010(3)	a = 8.13180(10), b = 15.9024(2) c = 11.0125(2)	a = 9.50760(10), b = 13.8415(2) c = 25.4627(4)
Cell angles	α = 90 β = 90 γ = 120	α = 90 β = 100.206(2) γ = 90	α = 90 β = 90 γ = 90	α = 90 β = 102.9067(8) γ = 90	α = 90 β = 90 γ = 90
Volume $Å^3$	6370.8(4)	1282.54(10)	1255.41(4)	1388.10(4)	3350.88(8)
Density (calculated)	1.151	1.177	1.752	1.633	1.535
F(000)	2376	488	648	672	1552
Θ_{max}	27.030	30.052	27.857	27.851	29.984
Minimal/maximal Transmission integration	0.98/0.99	0.98/0.99	0.78/0.90	0.63/0.76	0.74/0.83
μ	0.076	0.073	2.537	2.292	1.913
Total number of reflection	42363	13891	11348	12373	27364
Independent reflections (merging r)	1641 (0.089)	3732 (0.029)	2995 (0.082)	3309 (0.042)	4882 (0.079)
Data/restraints/parameters	949/0/99	2058/0/154	2006/5/155	2445/0/154	2623/0/181
Goodness of fit on F^2	0.9865	1.0045	0.8873	0.9961	0.9759
Reflection threshold expression	I>1.00u(I)	I>2.0u(I)	I>3.00u(I)	I>3.00u(I)	I>3.00u(I)
R indice (observed data)	0.801	0.0487	0.0272	0.0241	0.0293
wR indice (all data)	0.1189	0.0766	0.0250	0.0282	0.394
Minimal/maximal residual electron density	-0.23/0.60	-0.25/0.25	-0.58/0.59	-0.52/0.51	-0.60/0.53

Compounds	**1a**	**2a**	**2b**
Chemical formula	$C_{12}H_{15}N_1O_3$	$C_{20}H_{27}N_1O_1$	$C_{21}H_{29}N_1O_1$
Formula weight	221.26	297.44	311.47
Crystal appearance	Colourless plate	Colourless plate	Colourless plate
Size mm^3	0.02·0.14·0.22	0.20·0.30·0.34	0.10·0.13·0.22
Crystal system	Monoclinic	Orthorhombic	Orthorhombic
Space group	P 21/a	P21 21 21	P 21 21 21
Unit cell dimensions Å	a = 7.1003(2)	a = 9.4312(2)	a = 9.5331(2)
	b = 11.6103(3)	b = 10.3423(2)	b = 10.5986(2)
	c = 13.2476(4)	c = 18.2784(3)	c = 17.9101(4)
Cell angles	α = 90	α = 90	α = 90
	β = 100.6639(14)	β = 90	β = 90
	γ = 90	γ = 90	γ = 90
Volume $Å^3$	1073.23(5)	1782.88(6)	1809.59(7)
Density (calculated)	1.369	1.108	1.143
F(000)	472	648	680
Θ_{max}	27.487	27.457	27.455
Minimal/maximal Transmission integration	0.99/1.00	0.98/0.99	0.99/0.99
μ	0.099	0.067	0.069
Total number of reflection	7809	11641	12111
Independent reflections	2458	2328	2363
(merging r)	(0.018)	(0.044)	(0.040)
Data/restraints/parameters	1689/0/161	1651/0/200	1685/0/209
Goodness of fit on F^2	1.1445	1.507	1.1250
Reflection threshold expression	I>1.50u(I)	I>2.5\s(I)	I>2.4\s(I)
R indice (observed data)	0.0386	0.0320	0.0301
wR indice (all data)	0.0524	0.0479	0.0529
Minimal/maximal residual electron density	-0.19/0.25	-0.11/0.14	-0.12/0.14

Table 4: Crystal data and structure refinement for studied compounds.

Acknowledgments

The authors are indebted to the Région Alsace and the Programme Interreg III A Rhenaphotonics for their financial supports. We would like to gratefully acknowledge Dr. Albert Defoin for his valuable help in guiding this research work and for numerous fruitful comments and Prof. S. Walter for valuable comments during the preparation of the manuscript.

References

1. Albert, I. D. L.; Marks, T. J.; Ratner, M. A. *J. Am. Chem. Soc.* **1997**, *119*, 3155-3156.
2. Albert, I. D. L.; Marks, T. J.; Ratner, M. A. *J. Am. Chem. Soc.* **1998**, *120*, 11174-11181.
3. Pati, S. K.; Marks, T. J.; Ratner, M. A. *J. Am. Chem. Soc.* **2001**, *123*, 7287-7291.
4. Kang, H.; Facchetti, A.; Zhu, P.; Jiang, H.; Yang, Y.; Cariati, E; Righetto, S.; Ugo, R.; Zuccaccia, C.; Macchioni, A.; Stern, C. L.; Liu, Z.; Ho, S.-T.; Marks, T. J. *Angew. Chem. Int. Ed*. **2005**, *44*, 1-5.
5. Brown, E. C.; Marks, T. J.; Ratner, M. A. *J. Phys. Chem. B* **2008**, *112*, 44-50.
6. Fort, A.; Boeglin, A.; Mager, L.; Amyot, C.; Combellas, C.; Thiébault, A.; Rodriguez, V. *Synth. Met.* **2001**, *124*, 209-211.
7. Zalesny, R.; Bartkowiak, W.; Stryrcz, C.; Leszczynski, J. *J. Phys. Chem. A* **2002**, *106*, 4032-4037.
8. Boeglin, A.; Fort, A.; Mager, L.; Combellas, C.; Thiébault, A.; Rodriguez, V. *Chem. Phys.* **2002**, *282*, 353-360.
9. Niewodniezanski, W.; Bartkowiak, W. *J. Mol. Model.* **2007**, *13*, 793-800.
10. Boeglin, A.; Barsella, A.; Fort, A.; Mançois, F.; Rodriguez, V.; Diemer, V.; Chaumeil, H.; Defoin, A.; Jacques, P.; Carré, C. *Chem. Phys. Lett.* **2007**, *442*, 298-301.
11. Kang, H.; Facchetti, A.; Stern, C. L.; Rheingold, A. L.; Kassel, W. S.; Marks, T. J. *Org. Lett.* **2005**, *7*, 3721-3724.
12. Kang, H.; Facchetti, A.; Jiang, H.; Cariati, E.; Righetto, S.; Ugo, R.; Zuccaccia, C.; Macchioni, A.; Stern, C. L. Liu, Z.; Ho, S.-T.; Brown, E. C.; Ratner, M. A.; Marks, T. J. *J. Am. Chem. Soc.* **2007**, *129*, 3267-3586.
13. Marks, T. J.; Kang, H. US patent, US2006/0237368 A1.
14. Vonlanthen, D.; Mishchenko, A.; Elbing, M.; Neuburger, M.; Wandlowski, T.; Major, M. *Angew. Chem. Int. Ed*. **2009**, *48*, 8886-8890.
15. Duvanel, G.; Grilj, J.; Chaumeil, H.; Jacques, P.; Vauthey, E. *Photochem. Photobiol. Sci.* **2010**, *9*, 908-915.
16. Chaumeil, H.; Jacques, P.; Diemer, V.; Le Nouën, D.; Carré, C. *J. Mol. Struc.* **2011**, *1002*, 70-75.
17. Jacques, P.; Graff, B.; Diemer, V.; Ay, E.; Chaumeil, H.; Carré, C.; Malval, J.-P. *Chem. Phys. Lett.* **2012**, *531*, 242-246.
18. Diemer, V.; Chaumeil, H.; Defoin, A.; Fort, A.; Boeglin, A.; Carré, C. *Eur. J. Org. Chem.* **2006**, 2727-2738.
19. Diemer, V.; Chaumeil, H.; Defoin, A.; Fort, A.; Boeglin, A.; Carré, C. *Eur. J. Org. Chem.* **2008**, 1767-1776.
20. Diemer, V.; Chaumeil, H.; Defoin, A.; Boeglin, A.; Barsella, A.; Fort, A.; Carré, C.; *Proc. Spie-Org. Optoelectron. Photonics II* **2006**, *6192*, 559-565.
21. Barzoukas, M.; Fort, A.; Boy, P.; Combellas, C.; Thiébault, A. *Nonlinear Optics* **1994**, *7*, 41-52.

22. Barzoukas, M.; Fort, A.; Boy, P.; Combellas, C.; Thiébault, A. *Chemical Physics* **1994**, *185*, 65-74.

23. Runser, C.; Fort, A.; Barzoukas, M.; Combellas, C.; Suba, C.; Thiébault, A.; Graff, R.; Kintzinger, J.-P. *Chem. Phys.* **1995**, *193*, 309-319.

24. Rotzler, J.; Vonlanthen, D.; Barsella, A.; Boeglin, A.; Fort, A.; Mayor, M. *Eur. J. Org. Chem.* **2009**, 1096-1110.

25. Liu, L.; Xue, Y.; Wang, X.; Chu, X.; Yang, M. *Int. J. Quantum Chem.* **2012**, *112*, 1086-1096.

26. Allen, F. H.; Kennard, O.; Watson, D. G.; Brammer, L.; Orpen, G.; Taylor, R. *J. Chem. Soc. Perkin Trans. II*, **1987**, S1-S19.

27. Fabian, J.; Rosquete, G. A.; Montero-Cabrera, L. A. *J. Mol. Struct. THEOCHEM* **1999**, *469*, 163-176.

28. Marder, S. R.; Perry, J. W.; Tiemann, B. G.; Gorman, C. B.; Gilmour, S.; Biddle, S. L.; Bourhill, G. *J. Am. Chem. Soc.*, **1993**, *115*, 2524-2526.

29. Marder, S. R.; Gorman, C. B.; Tiemann, B. G.; Cheng, L.-T. *J. Am. Chem. Soc.*, **1993**, *115*, 3006-3007.

30. Marder, S. R.; Perry, J. W. *Adv. Mater.* **1993**, *5*, 804-815.

31. Gorman, C. B.; Marder, S. R. *Proc. Natl. Acad. Sci.* **1993**, *90*, 11297-11301.

32. Pinheiro, J. M. F.; de Melo, C. P. *J. Phys. Chem. A* **2011**, *115*, 7994-8002.

33. Kalaichelvan, S.; Sundaraganesan, N.; Dereli, O.; Sayin, U. *Spectrochimica Acta Part A* **2012**, *85*, 198-209.

34. Pastor, S. D. *J. Org. Chem.* **1984**, *49*, 5260-5262.

35. http//sdbs.db.aist.go.jp

36. Souchay, P.; Tatibouët, F.; Barchewitz, P. *J. Phys. Radium* **1954**, *15*, 533-535.

37. Altomare, A.; Cascarano, G.; Giacovazzo, G.; Guagliardi, A.; Burla, M. C.; Polidori, G.; Camalli, M. *J. Appl. Crystallogr.* **1994**, *27*, 435-436.

38. Betteridge, P. W.; Carruthers, J. R.; Cooper, R. I.; Prout, K.; Watkin, D. J. *J. Appl. Crystallogr.* **2003**, *36*, 1487.

39. Watkin, D.J.; Prout, C. K.; Pearse, L. J. *CAMERON*; Chemical Crystallography Laboratory: Oxford, UK, 1996.